A Numerical Study on the Effects of Nanoparticles and Stair Fins on Performance Improvement of Phase Change Thermal Energy Storages

M. E. Nakhchi[a], M. Hatami[b,1], M. Rahmati[a]

[a] Faculty of Engineering and Environment, Northumbria University, Newcastle upon Tyne, NE1 8ST, UK

[b] School of renewable energy and power engineering, Xi'an Jiaotong University, Xi'an, China

Abstract

Using nano-enhanced phase change materials is a widespread passive method to improve the melting performance, and also the storage capacity of the thermal energy storage units. In this study, the effects of CuO nanoparticles $(0 \le \phi \le 1.5\%)$ and new proposed stair fins on the efficiency improvement of latent heat thermal energy storage units are investigated. The stair fins are arranged in both upward and downward directions from the heated walls and the stair ratio is in the range of $0.67 \le b/c \le 4.0$. One of the vertical walls of the PCM enclosure is subject to uniform temperature and the other three walls are insulted. The numerical results show that by adding nanoparticles with volume concentration of $\phi = 1.5\%$ for b/c=0.67 to the flow, the energy storage capacity is enhanced by 9.1% compared to the pure PCM with downward fins. The maximum energy storage capacity of 474.1 kJ is achieved by using descending stair fins with b/c=4.0 and $\phi = 1.5\%$ which is much higher compared to the cases without nano additives. Besides, the melting performance is significantly improved by adding the nanoparticles. In fact, nanoparticles improve the thermal conductivity of the fluid and also act as a heat sink to absorb the heat from the fins. The downward fins with larger stair ratios (b/c=4.0) perform significantly better than the upwards ones which is because of the free convection effects and the recirculations flows on the upper face of these fins.

[1] Corresponding author, M. Hatami, Tel/Fax:+98-935-860-2679, E-mail: m.hatami@xjtu.edu.cn

Keywords: Nanoparticles; Phase change material; Thermal energy storage; Stair fins; Melting performance.

1. Introduction

Phase Change Materials (PCMs) are extensively used in thermal energy storages because they can collect or release thermal energy through the melting and freezing process of their phase exchange. Moreover, they can easily be used multiple times to save thermal energy. Due to this important characteristic, PCMs have many applications in energy storage, saving energy in buildings, solar systems, food industry, cooling and heat exchanger applications, reducing energy costs and providing thermal comfort in air conditioning and ventilation equipment. So, the PCMs usage has numerous advantages from the heat recovery, cost minimizing, energy saving, which can consequently lead to reductions in the use of fossil fuels.

Xu et al. [1] used the paraffin wax as triplex-layer phase change materials to investigate the storage performance in a latent heat thermal energy storage (LHTES) section numerically. They also employed metal fins with different inclination angles to have a faster heat transfer process. Pirasaci [2] applied the PCM into the exterior walls of the residential-apartment to investigate the heating and cooling process in different seasons and found that winter heating energy requirement is reduced by the PCM layer integrations. Another application of PCMs in building energy savings by using - encapsulated PCMs (Nano-PCM) and shape-stabilized PCMs is described by Wijesuriya et al. [3]. Also, Ručevskis et al. [4] presented a parametric study and design optimization of a PCM thermal energy storage system with active control for cooling buildings and reported that optimized cases could reduce the indoor air temperature by 9.5 ^{o}C, on average. Yang et al. [5] used a double PCM with suitable thermal properties using lauryl alcohol

and stearic acid with nanoparticles (LA-SA/Al_2O_3) for cooling and heating systems and found that 0.5% volume fraction of Al_2O_3 nanoparticles can improve the thermal conductivity of LA-SA by about 43%. Another study on the energy saving in buildings using various configurations and types of PCM is performed by Markarian and Fazelpour [6]. An electricity energy saving of 4.5–5.5% was observed for the climates and cities investigated in their study. Furthermore, Rathore et al. [7] experimentally investigated the effects of macro-encapsulated PCM on energy saving augmentation in buildings. They reported between 40% to 59% reduction in thermal amplitude, between 7 %-9% reduction in maximum temperature of all walls, and 38.76% reduction in cooling loads by using PCM in building walls and roof.

In addition to applications for energy saving in buildings, PCM has many applications in thermal energy storage (TES), photovoltaic thermal generators [8], thermoelectric generators [9], thermal control units (TCU) and solar still (SS) [10]. Solar applications of PCM in particular have received considerable attention in recent years by researchers due to its importance in renewable energy sector, in particular solar powered building and Solar-power plants. Recently, Palacio et al. [11] experimentally applied the PCM for a conventional flat plate solar collector (FPSC). They used two different PCMs, and solar collectors with different inclination angles for their analysis, from which they found that the thermal efficiency can increase from 26% to 28% for these cases. Vigneswaran et al. [12] performed an experimental study to investigate the thermal performance of three different passive solar stills with zero, one, or two PCMs. Their results show that the efficiency of solar still with one PCM is increased by 3.57% while the efficiency of the one with two PCMs by 7.57 % compared with the solar still with no PCM. Some of the researchers focused on the PCM applications in the heat exchangers due to their wide range of applications in industries. Mustafa et al. [13] and Mahdi et al. [14] used PCMs for double-pipe

helical-coil tube and shell and tube heat exchangers and examined the impact of different parameters on the melting process of PCMs.

One widespread method of thermal performance improvement is extended surfaces or fins method [15-17], while another one is nanoparticle additives approach [18-24]. There are some researches who have focused on using both these methods of thermal storage improvements, simultaneously [25]. The recent review study of Qiu et al. [26] showed that nano PCMs play a vital role in solar thermal energy storage systems. The performance of the solar TES units can significantly be improved by utilizing the nanoparticles. Sarani et al. [27] investigated the effects of fins and nanoparticles on PCM solidification and energy storage numerically and found that applied discontinuous fins can recover the energy release time by 89% and 84% compared with continuous copper and aluminum fins, respectively. Kok [28] also examined the effect of fins and nanoparticles on the PCM energy storage efficiency, experimentally. He used Al2O3 and CuO nanoparticles in paraffin wax and observed that using CuO nano-PCM can improve the melting performance of LHTES unit.. Recently, Arıcı et al. [29] also investigated the PCM melting performance by interior fins and CuO nanoparticles which revealed that the modified fins can increase the melting rate up to 52%. Gürtürk and Kok [30] and the Nóbrega et al. [31] investigated the fins effect on PCM melting process both experimentally and numerically. They proposed special fins to improve the PCM melting in non-melted regions in TES system. Another study on the fins arrangement and metal foam effects on PCMs is performed by Zhao et al. [32], which shows a 60% reduction in melting time can be achieved based on optimizing the number of fins. Santos et al. [33] enhanced the PCM solidification through finned pipes, and developed the correlations to examine PCM thermal performance. They also proposed new correlations to predict the melting interface within 4% error. Also, Li et al. [34] investigated the

effects of dispersing nano additives together with the insert of fins in solidification process and show that the longest fins and platelet shape nanomaterial had the fastest solidification process. Sathe and Dhoble [35] applied the inclined finned rectangular container in solar heat sinks fitted with external fins, and investigated the inclination angle effects on the thermal efficiency improvement. They showed that melting time increased with a decrease in inclination angles and the addition of fins number for all the PCM systems. Metal-oxides as potential nano-additives for paraffin in thermal storage applications are utilized by Khan et al. [36]. This study revealed that increasing the nanoparticles volume fraction will improve the charging rate of the melted PCM. For instance, the charging rate enhancement of SiO_2 NE-PCM with 1% and 5% volume concentrations were around 29% and 41%, respectively. Nakhchi and Esfahani [37] employed the stepped fins for improving the efficiency of the PCM LHTES systems. Their simulations confirmed that their proposed stepped fins had a faster melting process than the typical horizontal fins inside LHTES units. A recent study of Ji et al. [38] revealed that using inclined fins can improve the melting performance and the capacity of the energy storage systems. However, they only used fins without stairs in their study. Only a few studies focused on using inclined fines on performance augmentation of LHTES systems.

The above literature review illustrates that, although researches on latent heat storage (LHS) units have been performed in the past few years, there are no numerical or experimental studies to investigate the effects of using inclined fins, vertical heated walls, and nanoparticle additives simultaneously to improve the thermal energy storage efficiency. This motivates us to propose novel stair fins to utilize the advantages of both inclined fins and vertical walls at the same time. Moreover, using nanoparticle additives is employed to improve the efficiency of energy storage equipment. In the present study, performance improvement of latent heat thermal energy storage

units using both newly designed stair fins and nanoparticles will be investigated to find the most appropriate design for the stair fins. A common PCM, lauric acid, is used with Al_2O_3 nanoparticles as additives in this study. The effects of design parameters on the melting performance and the temperature distribution inside a rectangular enclosure are numerically investigated. The impact of the natural convection on the melting process is thoroughly discussed by utilizing the enthalpy-porosity method. Finally, the average power and thermal storage capacity for different fin geometries and nanoparticles volume fraction, together with thermoeconomic analysis are provided.

2. Physical description

Fig. 1 shows the schematic view of the LHTES enclosure fitted with three stair fins. The enclosure is filled with Lauric acid enhanced with CuO nanoparticles. The selected PCM has good latent heat with excellent chemical sustainability. The height of the enclosure (L) is kept constant at 120 mm with the width (D) of 50 mm. The right wall was isothermally heated at 333K and the other three walls are insulated. The initial temperature of the nano-enhanced PCM is 300K. The stair ratios of the fins are varied from 0 (horizontal fin) to 4 in both upward and downward directions. The details of the geometrical parameters are provided in Table 1. The thickness of the stair fins (δ) is varied between 1 to 3mm. The fins are made from aluminum plates with 5mm thickness (λ). The simulations are performed for three different numbers of fins (2-4) with different fin spacing (s). The details of the thermophysical properties of the selected materials are illustrated in Table 2. Lauric acid is selected as the main PCM material and CuO nanoparticles with different volume fractions are the additives in the main PCM fluid.

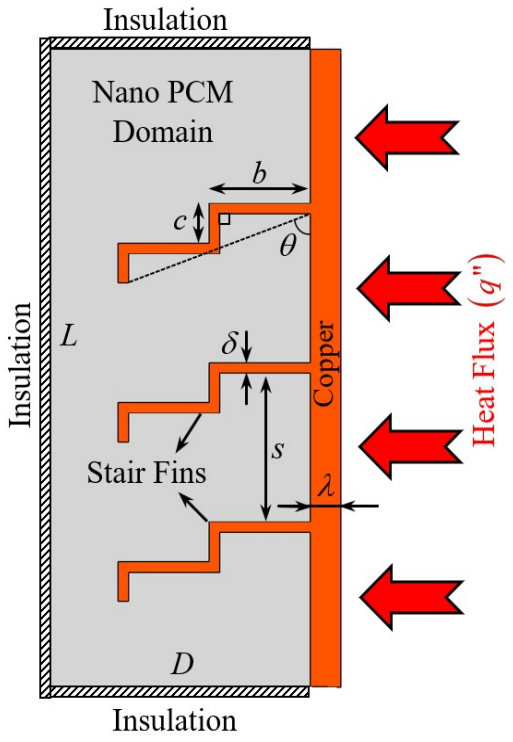

Fig. 1 Schematic of the LHTES unit with stair-fins and by nano-enhanced PCM domain.

Table 1 details of the various fin geometries.

Stair width (b), mm	Stair height (c), mm	θ, degree	Stair ratio (b/c)	Fin type
25.0	0	0	0	Straight fins
10.0	15.0	33.7	0.67	Down/Up
12.5	12.5	45.0	1.0	Down/Up
15.0	10.0	56.3	1.50	Down/Up
17.5	7.5	66.8	2.33	Down/Up
20.0	5.0	76.0	4.0	Down/Up

Table 2 Thermophysical properties of nano-enhanced lauric acid and aluminum [39-41].

Properties [units]	Lauric acid (solid/liquid)	CuO nanoparticles	Al
Melt temp. [°K]	316.5/321.2	-	-
C_p [J.kg^{-1}K^{-1}]	2180/2390	0.540	0.87
Latent heat [J.kg^{-1}]	187200	-	-
ρ [kg.m^{-3}]	940.0/885.0	6500	2719
k [W.m^{-1}K^{-1}]	1.6×10^{-1} -1.4×10^{-1}	18.0	202.4
β [K^{-1}]	8×10^{-4}	8.5×10^{-6}	-

Viscosity (μ) [Pa.s]	$\mu = \exp\left(\frac{1968}{T+273.15} - 4.25\right)$	-	-

3. Mathematical formulation

In this study, the enthalpy-porosity method within Ansys Fluent 19.3 software is employed for the numerical simulations. This method has been widely employed in the melting performance evaluation of PCMs in energy storage units [42]. Based on this method, different phase is assumed as porous media with the porosity of the fluid portion the whole domain.

This method utilizes various phases as a porous medium in which, porosity is identical to the PCM contribution in the model, and it is varied from 0 (solidus) to 1 (liquidus). Besides, the Boussinesq assumption is utilized for the buoyancy force evaluations. The governing equations for the two-dimensional, transient and incompressible nano-PCM flows in an enclosure can be expressed by [41]

- Mass conservation:

$$\frac{\partial \rho}{\partial t} + \frac{\partial (\rho u)}{\partial x} + \frac{\partial (\rho v)}{\partial y} = 0 \tag{1}$$

- momentum

$$\frac{\partial u}{\partial t} + \left(u\frac{\partial u}{\partial x} + v\frac{\partial u}{\partial y} \right) = \frac{1}{\rho_{nf}} \left[-\frac{\partial P}{\partial x} + \frac{\partial}{\partial x}\left[\mu_{nf} \frac{\partial u}{\partial x} \right] + \frac{\partial}{\partial y}\left[\mu_{nf} \frac{\partial u}{\partial y} \right] \right] \tag{2}$$

$$\frac{\partial v}{\partial t} + \left(u\frac{\partial v}{\partial x} + v\frac{\partial v}{\partial y} \right) = \frac{1}{\rho_{nf}} \left[-\frac{\partial P}{\partial y} + \frac{\partial}{\partial x}\left[\mu_{nf} \frac{\partial v}{\partial x} \right] + \frac{\partial}{\partial y}\left[\mu_{nf} \frac{\partial v}{\partial y} \right] + \rho_{nf} (g\beta)_{nf} (T - T_m) \right] \tag{3}$$

Where *u, v, t, P* and *nf* are the velocity components in *x* and *y* directions, time, pressure and nanofluid, respectively. This source term in the mushy zone can be expressed as:

$$S = -\frac{[1-\lambda]^2}{\left[\lambda^3 + \varepsilon\right]} A_{mushy} V \tag{4}$$

where $A_{mushy} = 5 \times 10^6$ is mushy zone constant and $\varepsilon = 0.001$ is a small parameter to avoid zero divisions in the numerical simulations. The liquid fraction (λ) can be expressed as:

$$\Delta H = \lambda L \rightarrow \begin{cases} \lambda = 0 \ \text{ if } T < T_{solidus} \\ \lambda = \dfrac{T - T_{solidus}}{T_{liquidus} - T_{solidus}} \ \text{ if } T_{solidus} < T < T_{liquidus} \\ \lambda = 1 \ \text{ if } T > T_{liquidus} \end{cases} \tag{5}$$

- Energy equation [43]

$$\frac{\partial T}{\partial t} = \frac{k_{nf}}{\left(\rho c_p\right)_{nf}} \left[\frac{\partial^2 T}{\partial x^2} + \frac{\partial^2 T}{\partial y^2} \right] \tag{6}$$

The sensible enthalpy is defined as [44]:

$$h = h_{ref} + \int_{T_{ref}}^{T} c_p dT \tag{7}$$

The density and specific heat capacity of the nano-PCM material are computed by utilizing these equations [41]:

$$\rho_{nf} = (1-\phi)\rho_f + \phi\rho_p \tag{8}$$

$$\left(\rho c_p\right)_{nf} = (1-\phi)\left(\rho c_p\right)_f + \phi\left(\rho c_p\right)_p \tag{9}$$

Where the subscriptions p and f refer to the nanoparticles and fluid, respectively. The other thermo-physical properties (thermal conductivity, and expansion coefficient) of CuO-PCM can also be calculated as [41]:

$$k_{nf} = \frac{k_p + 2k_f - 2\phi\left(k_f - k_p\right)}{k_p + 2k_f + \phi\left(k_f - k_p\right)} k_f \tag{10}$$

$$\left(\rho\beta\right)_{nf} = \left(1-\phi\right)\left(\rho\beta\right)_f + \phi\left(\rho\beta\right)_p \tag{11}$$

In the present study, Semi-Implicit Method for Pressure Linked Equations (SIMPLE) algorithm is utilized for the analysis together with PRESTO! Scheme which is a well-known method in modelling free-convection heat transfer problems. The maximum number of the iterations at each time step is 75. Moreover, second-order upwind scheme is utilized to discretize the governing equations, while second-order implicit scheme is also utilized for temporal discretizing. The under-relaxation parameters for density, pressure, velocity, temperature, and LF are 0.9, 0.3, 0.68, 1 and 0.9, respectively. The convergency of the parameters are assumed to reach 10^{-6} for the mass and momentum equations, and 10^{-8} for the temperature equation.

Fig. 2 illustrates the grid independency study performed in the present work to select appropriate number of elements (N) and time step$\left(\Delta t\right)$. It can be seen that different number of elements (N=14801, 19365 and 26147) were employed in the present study to capture the liquid fraction of nano-enhanced PCM inside LHTES enclosure fitted with stair fins over time. It can be seen that the difference the liquid fraction between N=19365 and 26147 is around 0.16%, which is small and negligible. Therefore N=19365 is selected for further simulations. Before performing further simulations, it was necessary to find an appropriate time-step for the transient phase-change analysis of nano-enhanced PCM inside LHTES unit. The time-steps were selected in the range of times steps utilized in the numerical study of Karami et al. [45]. They employed horizontal fins inside thermal energy storage unit filled with lauric acid without nanoparticles additives. The size of the enclosure in their study was identical to the present numerical analysis $\left(50\times120mm\right)$.

Three different time steps of 0.03, 0.07 and 0.18sec were employed to find the required time step. By comparing the time of the total melting process (t_m), it was observed that the deviations in the melting time between the 0.03, 0.07sec time steps is 0.05%. Consequently, $\Delta t = 0.07$ sec is the most appropriate time step for both accurate prediction, and effective computational cost of the transient liquid fraction of the nano-PCM melting, and it is selected for further simulations.

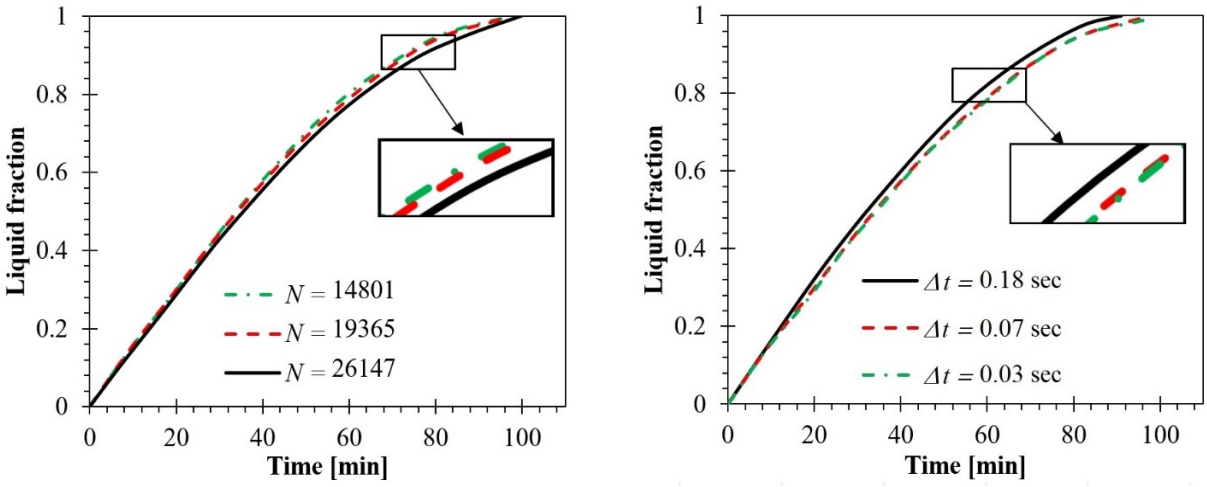

Fig. 2 grid and time-step independency study.

4. Results and discussion

4.1. Validation

for validation purposes the liquid fraction of the LHTS unit filled by lauric acid with 99% purity with three horizontal fins was compared with experimental and numerical data available in the literature. The comparisons were made for t= 900sec and 2700sec. It can be seen that the liquid fraction (LF) contours in this study agree with the previous studies inside enclosures equipped by typical horizontal fins with the same materials. This validation indicates that the present numerical results are trustworthy.

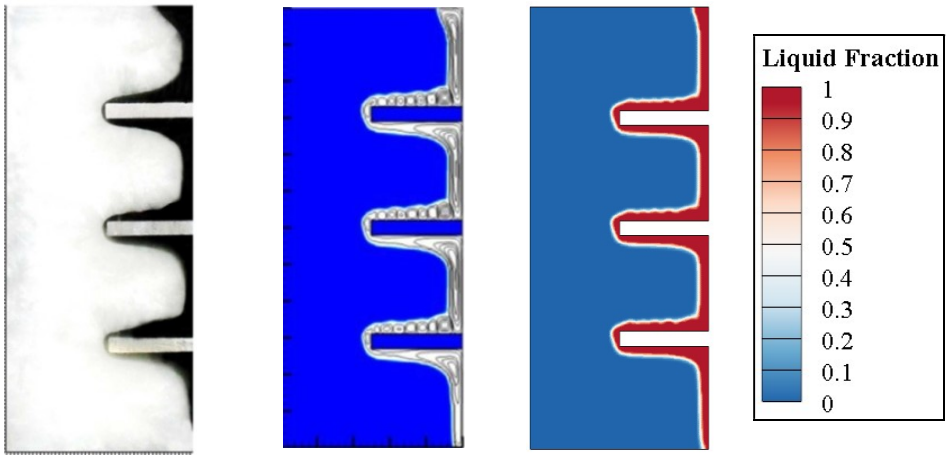

Kamkari et al. [46] (Exp.) | Karami et al. [45] (Num.) | Present study

a) t= 900 sec

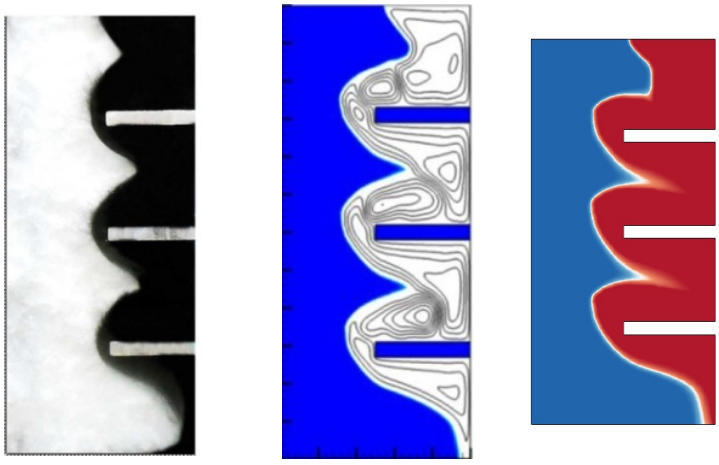

Kamkari et al. [46] (Exp.) | Karami et al. [45] (Num.) | Present study

b) t= 2700 sec

Fig. 3 Validation of the current numerical simulations with previous experimental and numerical studies on LHTES enhanced with three straight fins

To show the effect of downward and upward fins on the liquid fraction at different b/c ratios during time spending, Fig. 4 is depicted. As seen in this figure, for both upward and downward fins, PCMs starts to melt from the bottom and right corners, due to fins existence, then the melting is extended to the central section, and eventually shift at the top right corner to complete

the process, especially for upward fins. At initial time steps (t=1000sec) there is not a significant difference between the upward and downward fins, but at later times (t=4000sec) melting area for upward fins at the top of the enclosure is higher due to the natural convection flow arises with these fin geometries. This forces the flow upward due to decreasing the density caused by heated fins. It should be pointed out that the total melting time for downward stair fins is lower compared to the upward one (See Fig. 10). This lower melting time for the downward stir fins is mainly due to the more uniform temperature distribution inside the enclosure. The natural convection effects help to accelerate the melting process in the upper side, and the downward stair fins can intensify the melting speed in the lower side of the enclosure. The effect of the b/c ratio can be found from Fig. 4. As seen, for both upward and downward fins, for the small b/c ratio (0.67-1.0) melting process is fast at the beginning (t=1000sec), but it slows with increasing the melting process time (t=4000sec). This phenomenon can be explained by two main factors. Firstly, by increasing the b/c, the heated surface is increased, and consequently, more heat will transfer to PCM and melting will be faster. Secondly, lower b/c ratios make a region between the fins in which the fluid is trapped, due to natural convection in larger times. At the initial stage of melting process (at t=1000sec), however, this region helps to have more heat transfer and consequently faster melting.

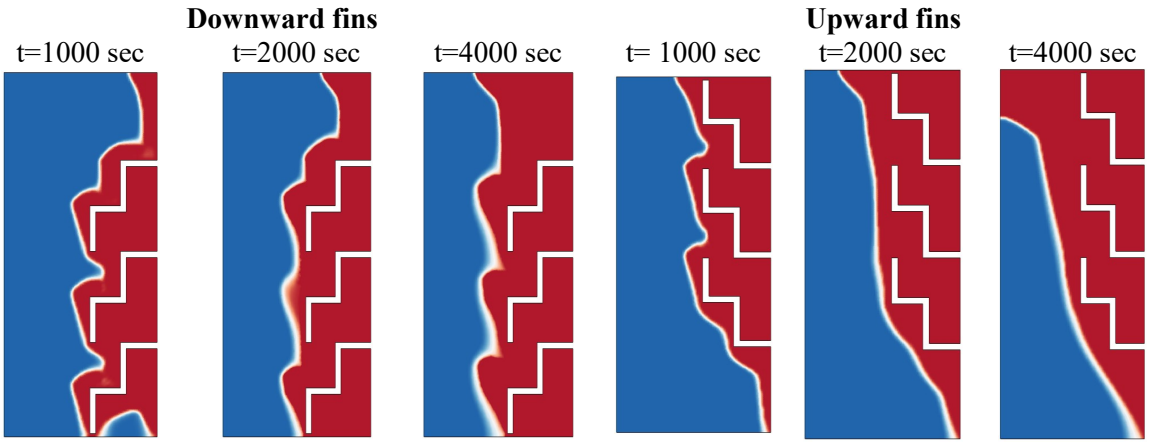

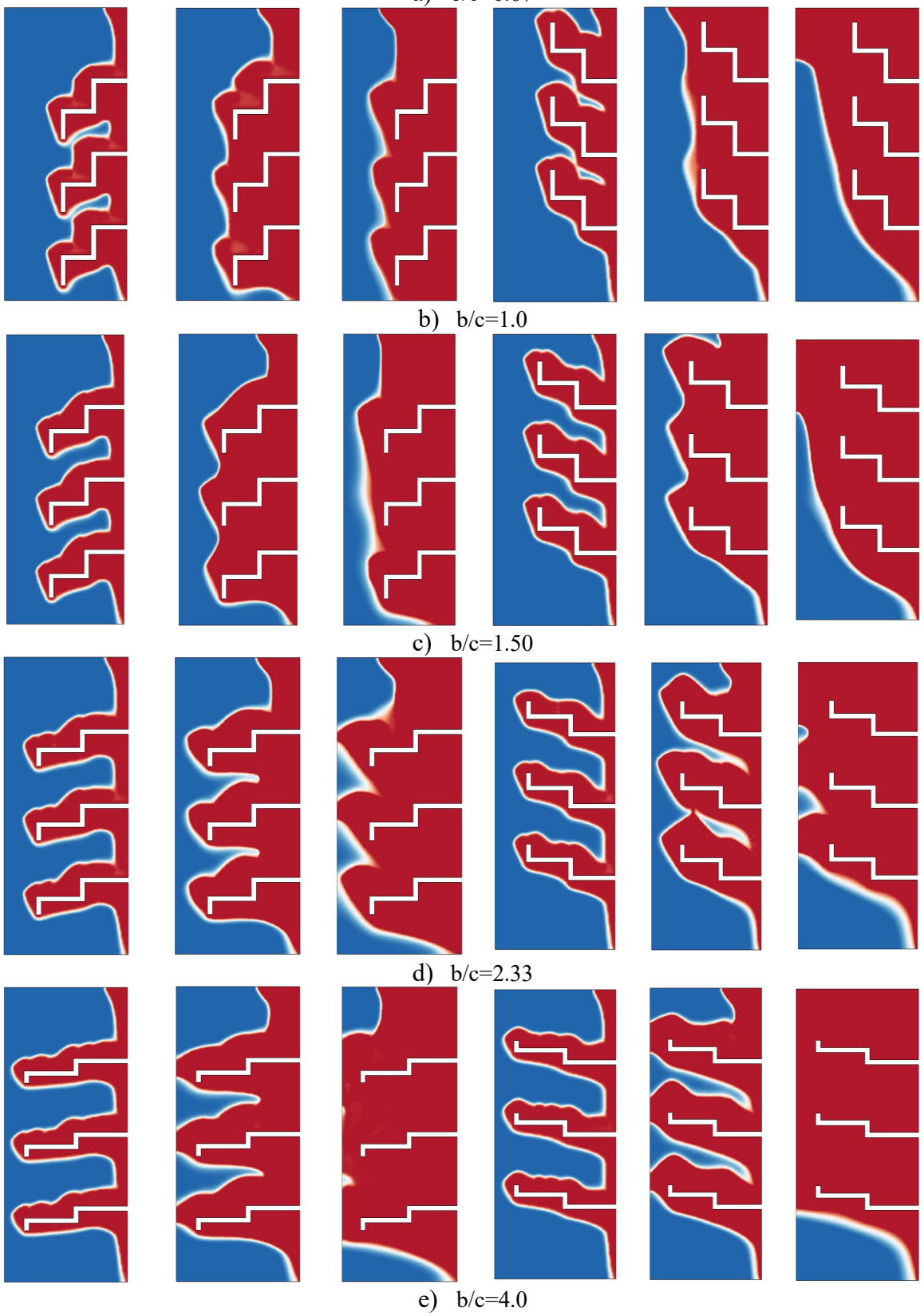
a) b/c=0.67
b) b/c=1.0
c) b/c=1.50
d) b/c=2.33
e) b/c=4.0

Fig. 4 Contours of liquid fraction inside stair-finned enclosure filled by nano-PCM material at different melting times for $\phi = 0.5\%$, $\delta = 2mm$.

Fig. 5 depicts the effects of fin spacing (s) on the melting process of nano-enhanced PCM inside LHTES enclosure fitted by downward stair fins with b/c=1.5. The results are presented for two different melting times (t=900 and 1800sec). It can be seen that the phase-change process significantly improved by using s=24 mm (N=4) compared to the other cases. In fact, using more fins can reduce the total melting time. However, using more fins reduces the PCM inside the enclosure which consequently reduces the energy storage capacity of the system. The vortex generations and recirculating flows near the junction between the horizontal and vertical fins can intensify the melting. Using four stair fins can reduce the total melting time up to 48% compared to the case with N=2.

The effects of fin thickness $(\delta = 1,2,3mm)$ inside latent heat thermal energy storage units filled with nano-PCM material on the total melting time is provided in Table 3. It can be seen that the melting time can be reduced by using thicker stair-fins. However, the storage capacity is reduced by utilizing the thicker fins, which is due to the smaller PCM capacity inside the enclosure. The results show that the total melting time can be reduced by 35.7% by raising the fins thickness from $\delta = 1mm$ to 3mm for b/c=4.0.

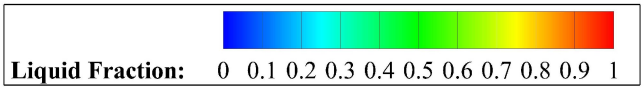

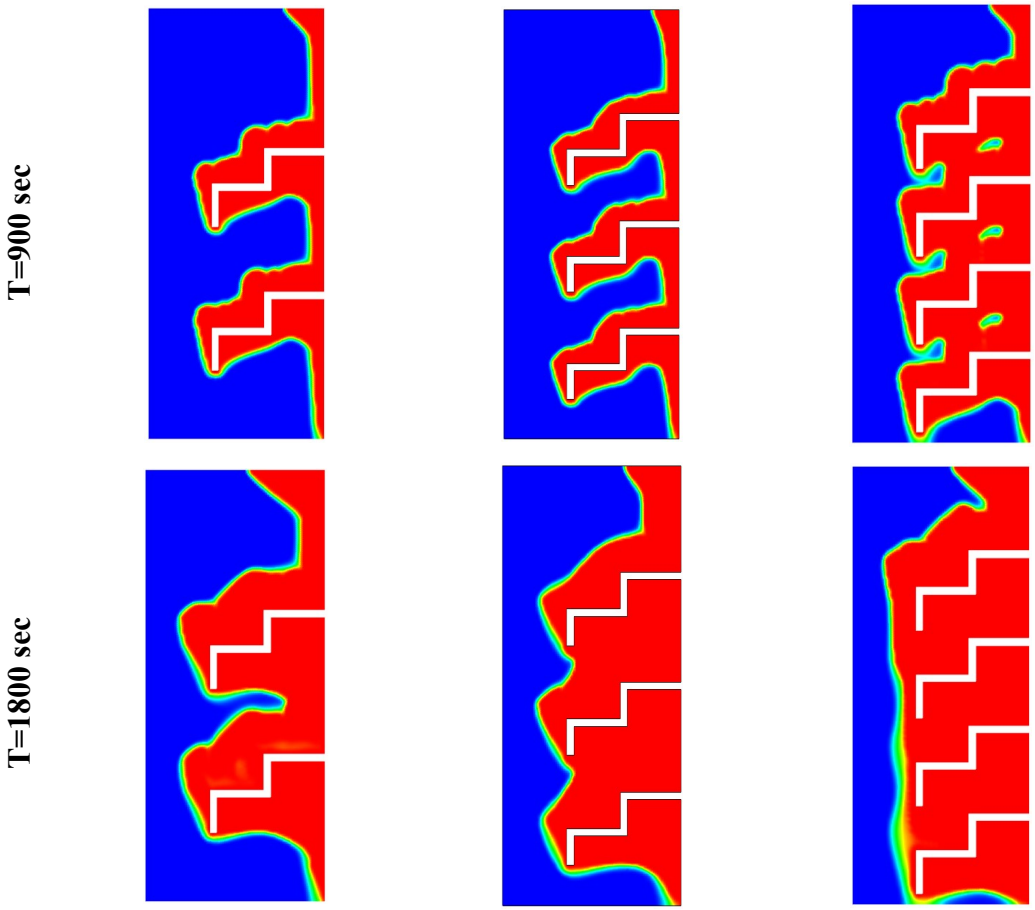

a) s=40 mm (*N*=2) b) s=30 mm (*N*=3) c) s=24 mm (*N*=4)

Fig. 5 The effects of fin spacing (s) on the melting performance inside LHTES enclosure filled with nano-PCM with downward stair fins (b/c=1.5, $\phi = 0.5\%$)

Table 3 The effects of fin thickness on total melting time (t_m) inside LHTES unit filled with nano-PCM $(\phi = 1\%)$ with different stair ratios.

Fin thickness	Total melting time (t_m), sec		
	b/c=1	b/c=1.5	b/c=4.0
$\delta = 1mm$	8122.14	6428.42	4866.02
$\delta = 2mm$	7228.95	5517.08	3968.40
$\delta = 3mm$	6321.80	4609.25	3128.53

Fig. 6 demonstrates the temperature contours for the discussed geometry of fins, upward and downward at different b/c ratios. Due to heated fins, it can be seen that greater temperatures occur around the fins. At the initial times (t=100, 400sec) there is no significant difference between the temperatures for upward and downward fins. However, at later stages (t=700, 1000sec) the temperatures around the downward fins is much greater than upward fins due to trapped region of heat at the bottom of fins, while for upward fins the fluid flows upward due to natural convection and lower density fluid. Fig. 6, shows that upward stair fins have more uniform temperature distributions because melted nano-PCM with high temperature flows to the upper side, easily without any obstacle (contrary to the downward stairs cases) due to the impacts of free convection. The main reason for the heat retention between the downward fins is that heat tends to move upward due to the natural convection. However, in the presence of downward fins heat will be trapped between the stair walls and the enclosure walls. However, in the upward fins, the heat can easily go up, because the vertical obstacle in the presence of the stair fins is removed.

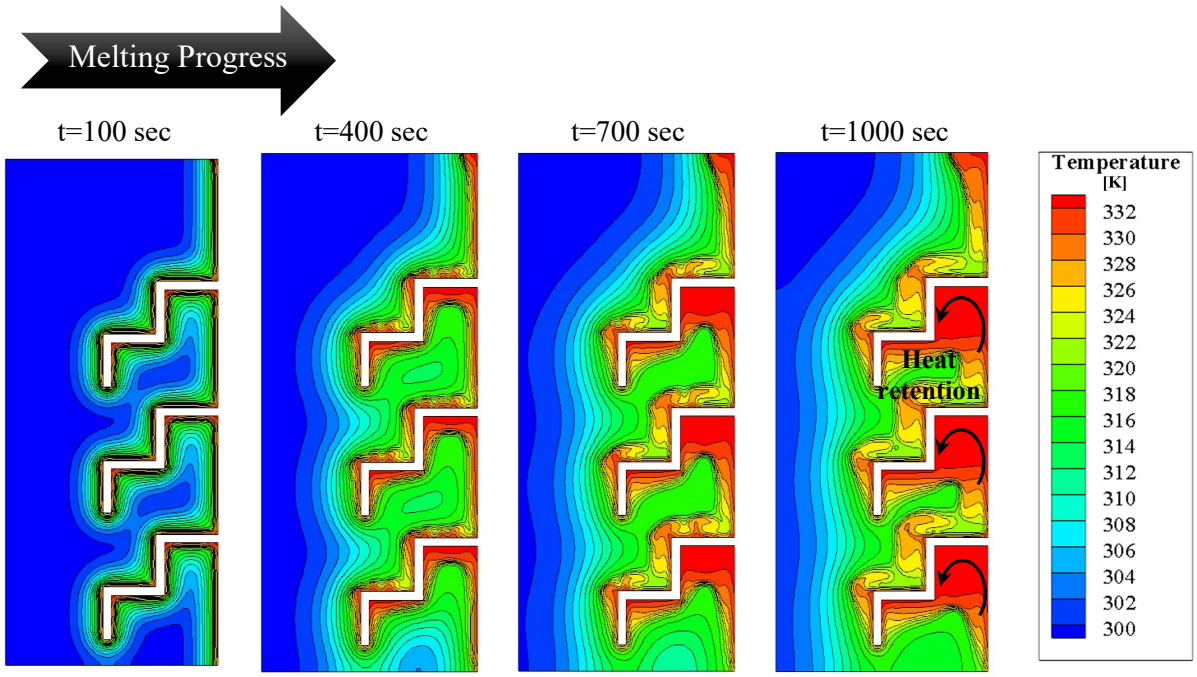

a) Downward stair fins

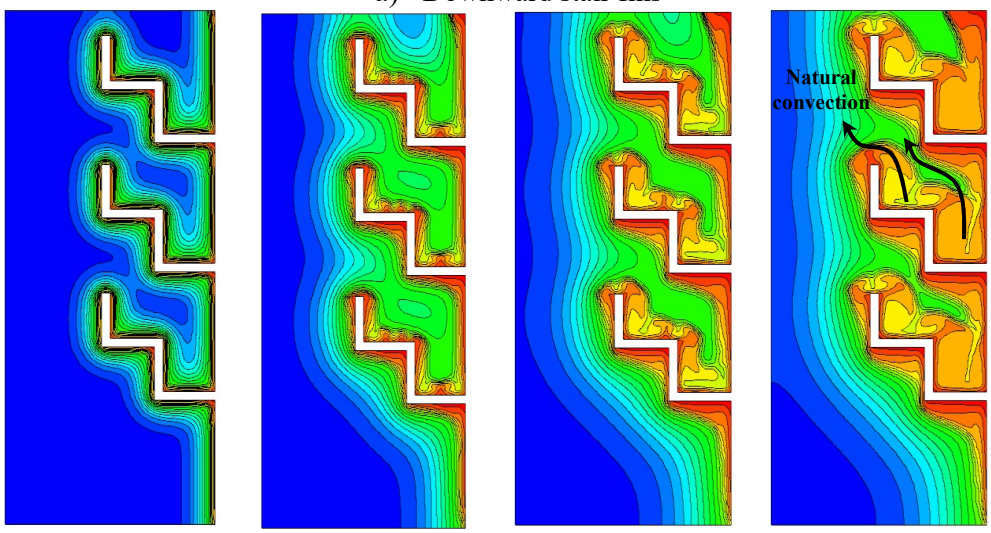

b) Upward stair fins

Fig. 6 Temperature contours inside downward and upward stair-finned enclosure filled by nano-PCM material at different melting times for $\phi = 0.5\%$, b/c=1.0.

Fig. 7 shows the effects of nanoparticles with different volume fraction on the melt fraction and temperature profiles at 600sec. As seen from the temperature contours, by increasing the nanoparticles volume fraction from 0 to 1.5% the melted area will increase due to higher thermal conductivity of nano-PCM and consequently, higher temperature around the fins. In fact, nanoparticles additives act as heat sinks and absorb the heat from fins, so it facilitates faster melting of PCM.

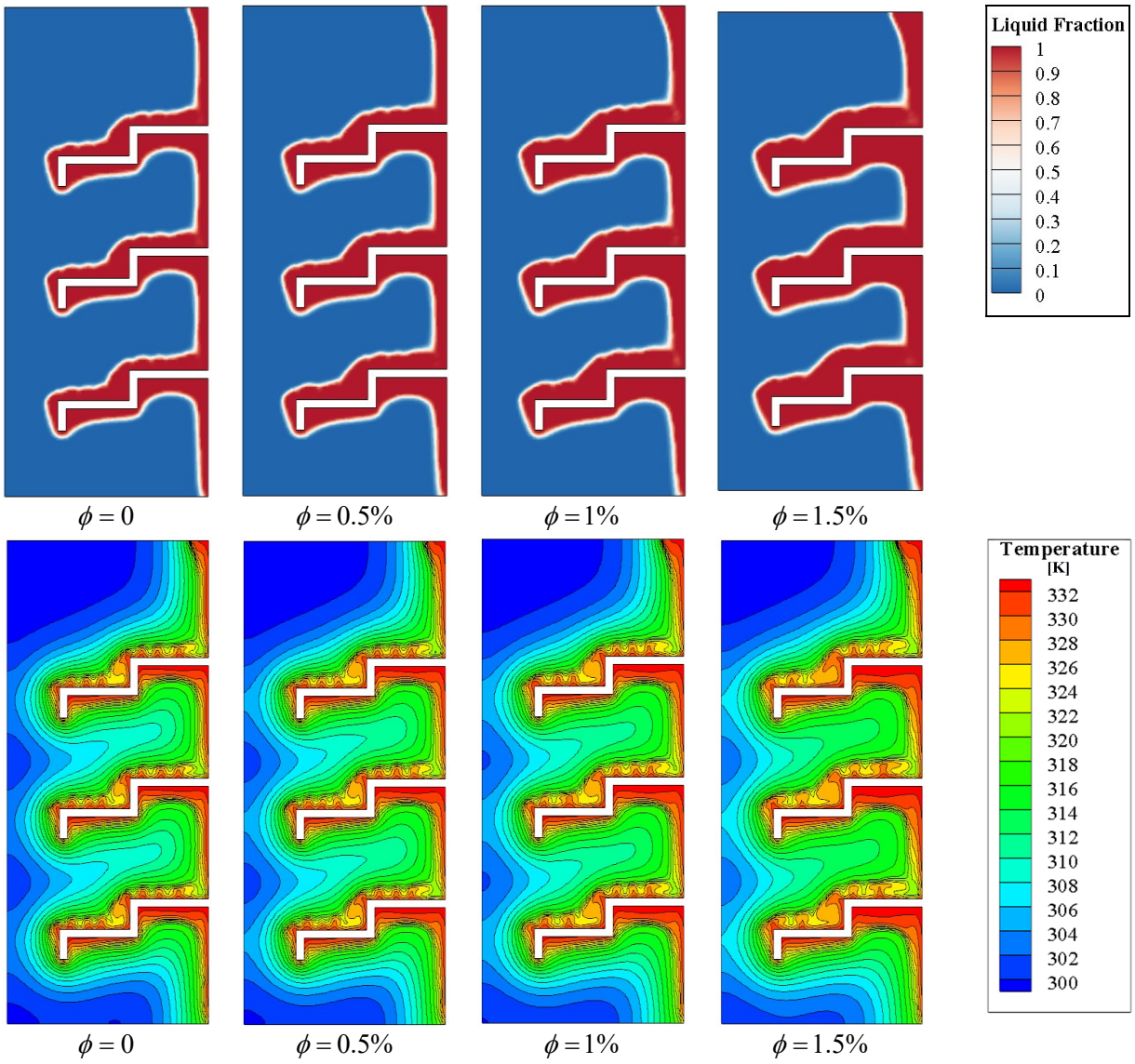

Fig. 7 The effects of nanoparticles volume fraction (ϕ) on the melting improvement inside stair-finned enclosures at t=600 sec.

Furthermore, nanoparticles make some recirculation zones, especially near the fin walls as presented in Fig. 8, which causes more turbulence and consequently, more heat transfer through these zones. These recirculation areas lead to a portion of the energy transported to the solid-liquid interface and make a faster and better melting process in storage energy systems. It can be deduced that these recirculation zones are stronger at higher melting process times (t=1500 sec). Consequently, heat transfer rate will increase with time due to stronger recirculation areas around

the heated surfaces. Heat naturally tends to go up, but the cold and frozen area above the molten material interacts with the melted PCM and thus, prevents heat flow toward the upstream direction. As a result, a vortex flow forms on the fins, which increases the mixing of the current between the fan wall and the phase change material.

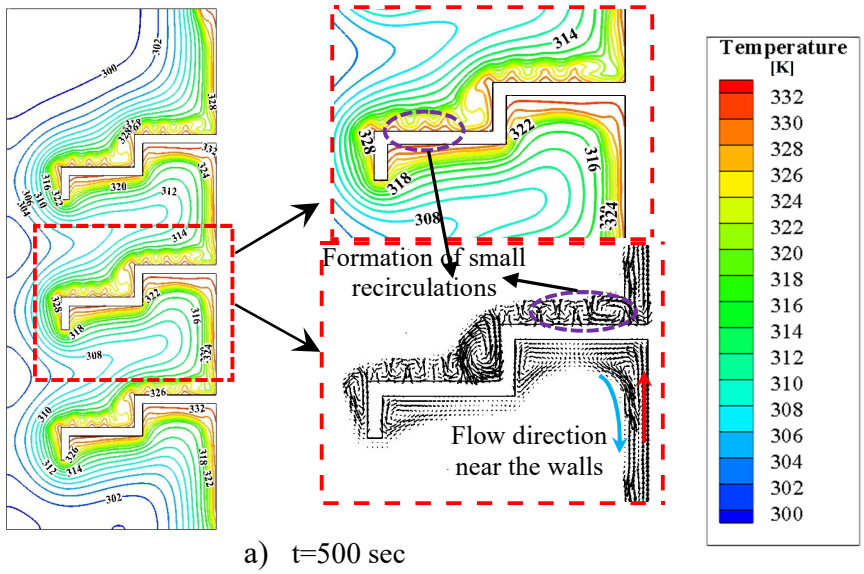

a) t=500 sec

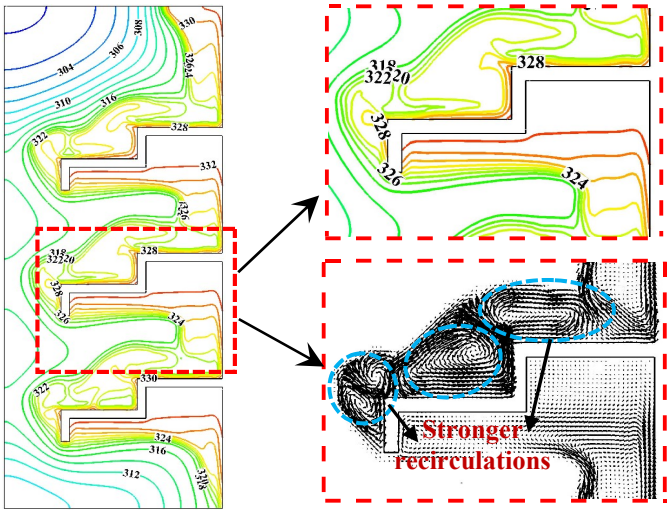

b) t=1500 sec

Fig. 8 Velocity vectors and recirculation flows over the stair fins at different melting times (b/c=2.33).

As mentioned above, the stair ratio (b/c) is one of the most critical parameters that affect the temperature distribution. This effect for nano-PCM is presented in Fig. 9 for t=1800sec. For lower b/c ratio (0.67), the temperature distribution is uneven due to heat retention between the fins and the enclosure insulated walls, which could not release in the whole enclosure domain. By increasing the b/c ratio up to 4.0, the heat propagation inside the enclosure becomes identical. Due to the natural convection flow, the temperatures distribution is more uniform. The results illustrate that the heat retention between the upward fins with b/c=0.66, and the enclosure upper makes the temperature distribution non uniform inside the energy storage unit. This has a negative effect on the energy saving efficiency inside the enclosure filled with nano-PCM material.

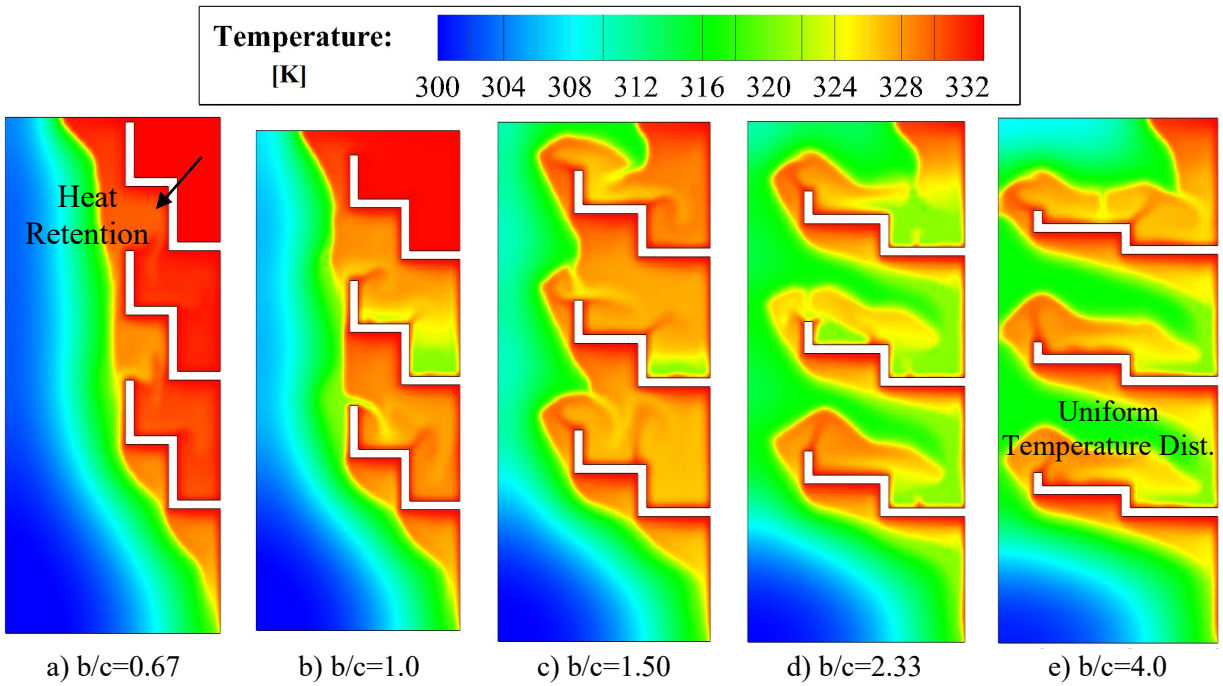

Fig. 9 The effects of stair ratio on the temperature distribution inside the nano enhanced PCM enclosure at t=1800 sec.

As seen in this Fig. 10, a comparison between different b/c ratios for upward and downward fin stairs is performed. In both fin configurations (upward and downward), by increasing the b/c ratios, the final melted mass fraction is enhanced due to enhanced heat transfer from larger fins and the absence of trapped heat areas. It is worth mentioning that at early stage of melting process an opposite behavior can be observed. It can be deduced that the total melting time for the case of downward fins with b/c-4.0 can be reduced by 16.7% compared to the upward fins with the same stair ratio. As discussed earlier, this is mainly due to the more uniform temperature distribution inside the enclosure in the presence of downward stair fins compared to the upward fins. The downward fins help the melting process in the lower areas of the enclosure, while the melting would be higher in the upper side due to the natural convection effects and the recirculating flows.

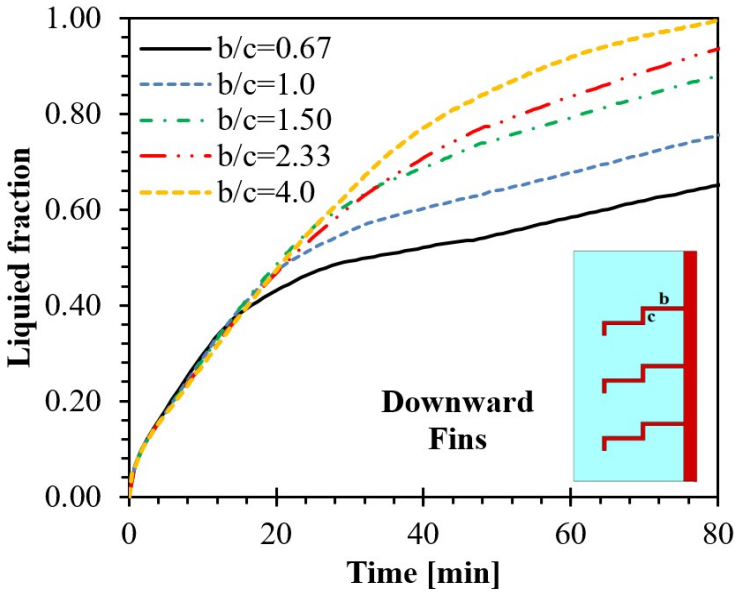

a) Downward stair fins

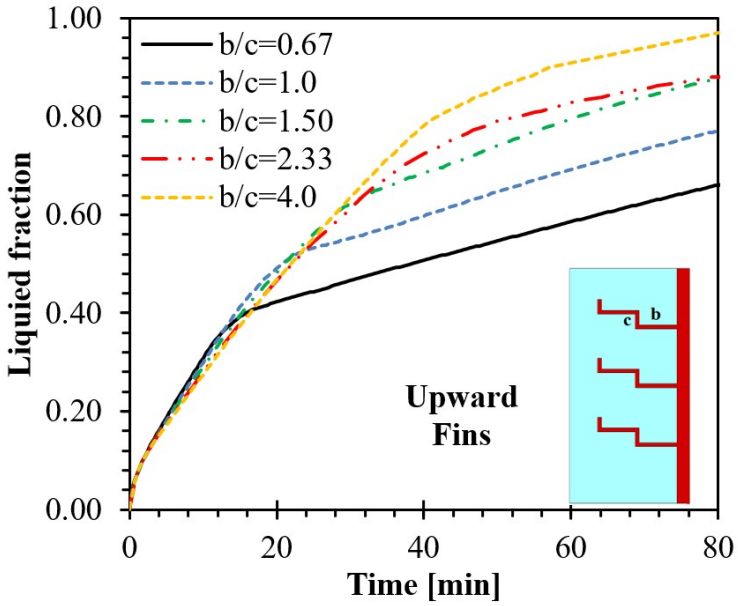

b) Upward stair fins

Fig. 10 The effects of step ratio (b/c) on liquid fraction versus time for upward and downward stair fins $(\phi = 1\%)$.

Fig. 11 confirms that using the nanoparticles enhances the melting process, significantly. Indeed, during the whole melting process time (0-80 min), greater nanoparticle volume fraction results in faster melting process which is due to better thermal conductivity and more heat transfer to PCM than smaller VF values. This behavior is also observed by other researchers, which approve the efficiency of using nanoparticles in these applications. As seen, when the φ=1.5%, 100% of PCM is melted after 80 min, while for φ=0%, approximately 85% of PCM is melted at the same time, so nanoparticle additives cause a faster melting process for PCM at thermal energy storages.

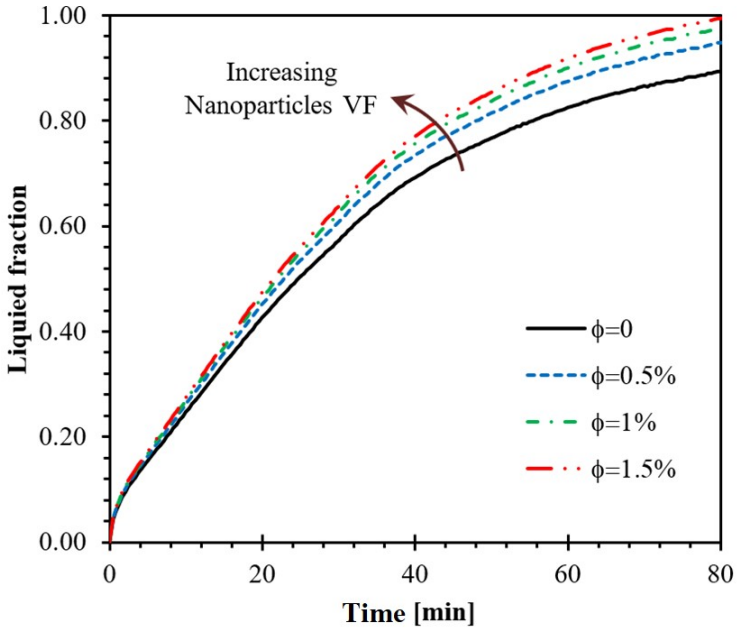

Fig. 11 The effects of nanoparticles volume fraction on melting performance inside LHTES unit fitted with downward stair-fins with b/c=4.0.

The wall heat flux inside LHTES units for both upward and downward and b/c=0.67 and 4.0 cases is presented in Fig. 12. In this figure, q" (t) can be described as $q"(t)= Q(t)/A$ where $Q(t)$ refers to the instant entire heat transfer rates to the PCM and A denotes the overall heat transfer surface as a sum of the base and fins. Approximately before t=16min, all the cases had a quick reduction in heat flux. Afterward, the behavior of the presented cases is different. Upward fins with b/c=0.67 have the minimum heat flux at larger times (t>16min). After that, downward fins with the same b/c ratio (0.67) presented lower heat flux. For the cases with b/c=4.0, it can be observed that a peak of heat flux is observed. This peak for the upward case occurs faster at 45min about 1350 W/m^2, so it makes a faster melting process compared to other presented cases.

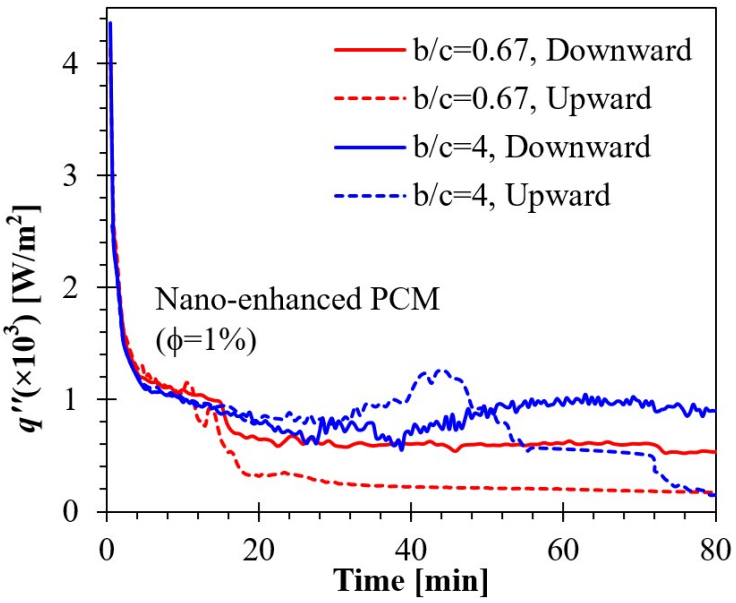

Fig. 12 The effects of stair fin geometry on wall heat flux inside LHTES units for different times.

Fig. 13 shows the effects of CuO nano additives on the mean temperature of the LHTES unit equipped with descending stair fins with various stair ratios. It is observed that the mean temperature rises up to 3.9° C by utilizing stair fins with larger ratios (b/c=4.0) compared to b/c=0.67 at a specific time. This is mostly because of the free convection effects and more uniform heat distribution inside the enclosure in the presence of the recirculation flows. The results show that the mean temperature could be augmented up to 8.1° C by using nano-PCM with $\phi = 1.5\%$ compared to the pure lauric acid at b/c=4.0. Adding the nanoparticles to the pure PCM, improves the thermal conductivity of the phase change material. Consequently, the heat propagates much faster inside the enclosure and the mean temperature goes up.

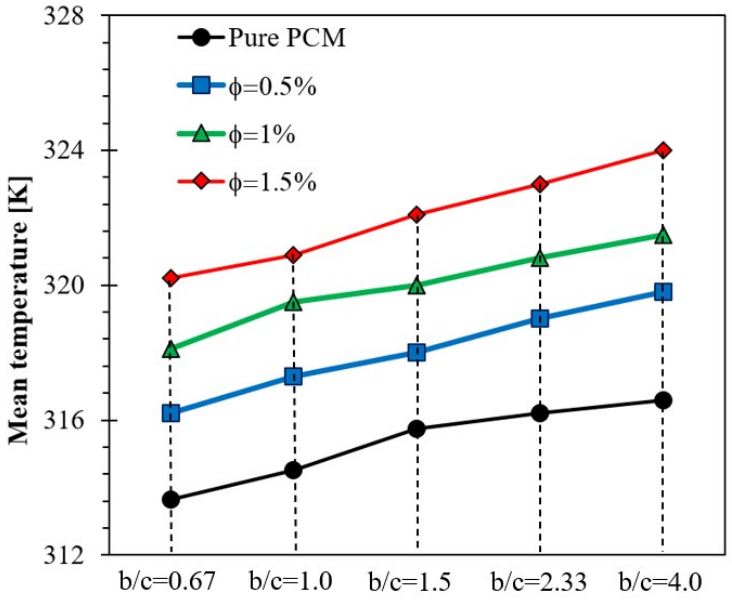

Fig. 13 The effects of the nanoparticles volume fraction on the mean temperature of nano-enhanced PCM with different stair-fin ratios.

The effects of CuO nanoparticles volume fraction on the energy storage capacity (ESC) of the LHTES unit equipped by stair-fins with various shapes are depicted in Fig. 14. The results are provided for the downward stair fins with various b/c values. As expected, the energy storage capacity enhanced around 9.1% by adding CuO nanoparticles with a volume concentration of $(\phi = 1.5\%)$ to the lauric acid for b/c=0.67. The results illustrate that the maximum energy storage capacity of 474.1 KJ could be achieved by using descending stair fins with b/c=4.0 and $\phi = 1.5\%$. The thermal energy storage capacity is improved 21.8%, 22.0%, 18.6% and 16.7 by raising the stair ratio from 0.67 to 4.0 for $\phi = 0$, 0.5, 1, and 1.5%, respectively. As discussed earlier, the melting performance of the LHTES enclosure can be improved significantly by using stair fins with larger stair ratios. This is due to the more uniform heat distribution inside the enclosure by utilizing downward fins.

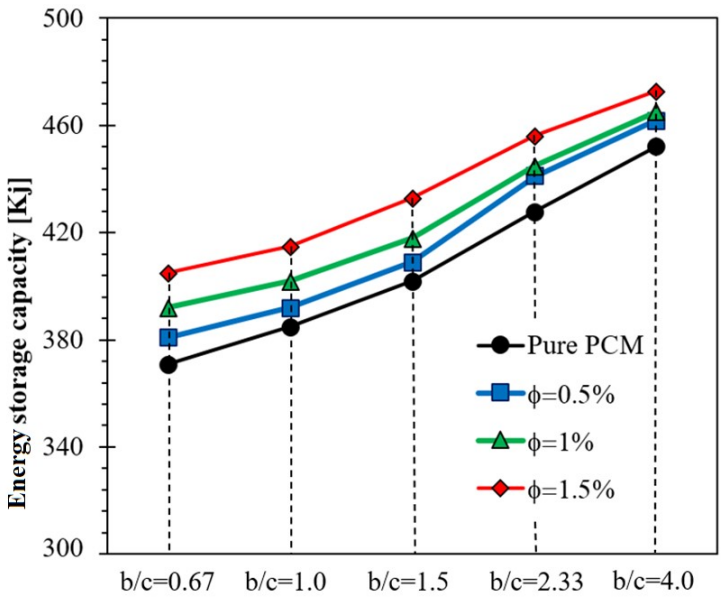

Fig. 14 The effects of the nanoparticles volume fraction on the energy storage capacity (ESC) inside LHTES unit with different stair-fin configurations.

4.2. Economic analysis

Selecting appropriate materials is an important parameter in the design of the latent heat thermal energy storage units. Performance improvement and economical requirements are the main two factors that should be considered in using nano enhanced PCM. The main objectives are having high efficiency together with low costs. For instance, some high thermal conductivity nanoparticles (Cu, CuO, etc.) are great additives in terms of the melting performance augmentation and the energy storage capacity, but these nanoparticles are very expensive compared to the other nano additives. Consequently, the amount of the nanoparticles used in the PCM can be an appropriate way to improve the energy saving and reducing the materials costs. For this purpose, a new parameter called thermal energy storage per material cost $\left(p_c\right)$ can be defined as [47]:

$$p_c = \frac{ESC}{t_m R} = \frac{m_p \int \left(c_p\right)_p dT + m_{PCM} \int \left(c_p\right)_{PCM} dT + L_h + m_p \int \left(c_{p,1}\right)_{PCM} dT}{t_m \left(a_p m_p + a_{PCM} m_{PCM}\right)} = \frac{m_{PCM} L_h}{t_m \left(a_p m_p + a_{PCM} m_{PCM}\right)} \quad (12)$$

where t_m, a, L_h, and m denote melting time (sec), material cost per unit ($/kg), latent heat (J/kg), and mass (kg). This parameter can be made dimensionless by dividing it to the material costs without using nanoparticles (pure PCM) as follows [47]:

$$p_c' = p_c / p_{c,0} = \frac{m_{PCM} L_h}{t_m \left(a_p m_p + a_{PCM} m_{PCM}\right)} \Bigg/ \frac{m_{PCM} L_h}{t_{m,0} a_{PCM} m_{PCM}} = \frac{m_{PCM}}{t_m / t_{m,0} \left(N m_p + m_{PCM}\right)} \quad (13)$$

In the above equation p_c', $N=a_p/a_{PCM}$, and subscript 0 denote dimensionless ESC rate per material cost, price ratio, and pure PCM case without nanoparticles. Influenced by the market variations the price ratio (N) can be changed. For the case of pure PCM melting without CuO nanoparticle additives, p_c' would be equal to unity.

Fig. 15 shows the variations of the p_c' with respect to the price ratio. It can be seen that using nanoparticles with different volume fractions significantly improves the economic efficiency up to 5-6 times compared to the case without nano additives $\left(\phi = 0\right)$. It can be seen that when N is smaller than 8 (cheaper nanoparticles), the price efficiency is the highest for the case of $\phi = 1.5\%$. This indicates that using cheaper nanoparticles with higher volume fractions is an appropriate approach for energy saving improvement of nano-PCM in LHTES units. However, the price efficiency becomes smaller by using more expensive nano additives. The efficiency is the highest for $\phi = 0.5\%$ when the price ratio (N) is larger than 15.

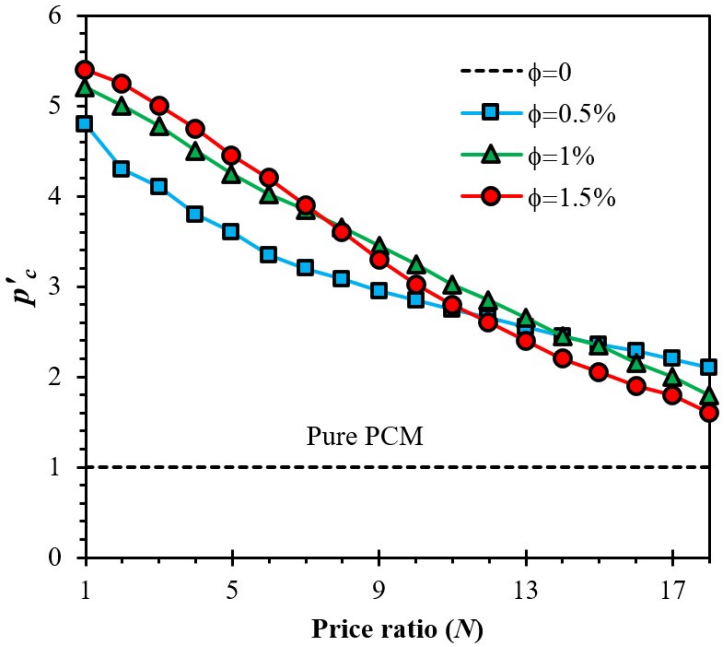

Fig. 15 Variations of p'_c with price ratio (N) for nano-enhanced PCM with different volume fractions for downward stair fins with b/c=1.5.

5. Conclusion

In this study, the melting performance and energy storage capacity of LHTES units filled by nano-PCM is numerically examined. The effects of CuO nanoparticles together with both downward and upward stair fins with different stair ratios on the performance characteristics, temperature distribution, and the melting time are investigated. The results are compared with typical horizontal fins to show the improvement of the proposed stair fins. The main findings are summarized as follows:

- Using nanoparticles together with stair fins can significantly improve the melting performance of the LHTES units. The vortex generation of the melted PCM near the stair fins can significantly improve the heat transfer inside the enclosure, which improves the

energy saving efficiency. Smaller stair ratios make a trapped region between the fins, which prevents the fluid from recirculation due to the natural convection.

- The effects of nanoparticles volume fraction and the stair ratio of the fins in both upward and downward directions were investigated. The energy storage capacity could be increased around 9.1% by adding CuO nanoparticles with volume fraction of $(\phi = 1.5\%)$ to the lauric acid for b/c=0.67.
- The maximum energy storage capacity of 474.1 KJ could be achieved by using downward stair fins with b/c=4.0 and $\phi = 1.5\%$.
- It can be seen that using nanoparticles with different volume fractions significantly improves the economic efficiency by up to 5-6 times compared to the case without nano additives $(\phi = 0)$. It can be seen that when *N* is smaller than 8 (cheaper nanoparticles), the price efficiency is the highest for the case of $\phi = 1.5\%$.
- For both upward and downward fins, for the small b/c ratios (0.67-1.0) the melting process is faster initially, but it becomes slower at later stages of the melting process time (t=4000 sec).
- By raising the stair ratio from 0.67 to 4.0, the thermal energy storage capacity is improved by 22.0% for $\phi = 1\%$..

References

[1] H. Xu, N. Wang, C. Zhang, Z. Qu, M. Cao, Optimization on the melting performance of triplex-layer PCMs in a horizontal finned shell and tube thermal energy storage unit, Applied Thermal Engineering, (2020) 115409.
[2] T. Pirasaci, Investigation of phase state and heat storage form of the phase change material (PCM) layer integrated into the exterior walls of the residential-apartment during heating season, Energy, (2020) 118176.

[3] S. Wijesuriya, P.C. Tabares-Velasco, K. Biswas, D. Heim, Empirical validation and comparison of PCM modeling algorithms commonly used in building energy and hygrothermal software, Building and Environment, 173 (2020) 106750.
[4] S. Ručevskis, P. Akishin, A. Korjakins, Parametric Analysis and Design Optimisation of PCM Thermal Energy Storage System for Space Cooling of Buildings, Energy and Buildings, (2020) 110288.
[5] Y. Yang, W. Wu, S. Fu, H. Zhang, Study of a novel ceramsite-based shape-stabilized composite phase change material (PCM) for energy conservation in buildings, Construction and Building Materials, 246 (2020) 118479.
[6] E. Markarian, F. Fazelpour, Multi-objective optimization of energy performance of a building considering different configurations and types of PCM, Solar Energy, 191 (2019) 481-496.
[7] P.K.S. Rathore, S.K. Shukla, An experimental evaluation of thermal behavior of the building envelope using macroencapsulated PCM for energy savings, Renewable Energy, 149 (2020) 1300-1313.
[8] F. Rajaee, M.A.V. Rad, A. Kasaeian, O. Mahian, W.-M. Yan, Experimental analysis of a photovoltaic/thermoelectric generator using cobalt oxide nanofluid and phase change material heat sink, Energy Conversion and Management, 212 (2020) 112780.
[9] C. Selvam, S. Manikandan, N.V. Krishna, R. Lamba, S. Kaushik, O. Mahian, Enhanced thermal performance of a thermoelectric generator with phase change materials, International Communications in Heat and Mass Transfer, 114 (2020) 104561.
[10] L. Yang, J.-n. Huang, F. Zhou, Thermophysical properties and applications of nano-enhanced PCMs: An update review, Energy Conversion and Management, 214 (2020) 112876.
[11] M. Palacio, A. Rincón, M. Carmona, Experimental comparative analysis of a flat plate solar collector with and without PCM, Solar Energy, 206 (2020) 708-721.
[12] V. Vigneswaran, G. Kumaresan, B. Dinakar, K.K. Kamal, R. Velraj, Augmenting the productivity of solar still using multiple PCMs as heat energy storage, Journal of Energy Storage, 26 (2019) 101019.
[13] M.S. Mahdi, H.B. Mahood, J.M. Mahdi, A.A. Khadom, A.N. Campbell, Improved PCM melting in a thermal energy storage system of double-pipe helical-coil tube, Energy Conversion and Management, 203 (2020) 112238.
[14] J.M. Mahdi, H.I. Mohammed, E.T. Hashim, P. Talebizadehsardari, E.C. Nsofor, Solidification enhancement with multiple PCMs, cascaded metal foam and nanoparticles in the shell-and-tube energy storage system, Applied Energy, 257 (2020) 113993.
[15] M. Hatami, M. Jafaryar, D. Ganji, M. Gorji-Bandpy, Optimization of finned-tube heat exchangers for diesel exhaust waste heat recovery using CFD and CCD techniques, International Communications in Heat and Mass Transfer, 57 (2014) 254-263.
[16] M. Hatami, D. Ganji, M. Gorji-Bandpy, Experimental and numerical analysis of the optimized finned-tube heat exchanger for OM314 diesel exhaust exergy recovery, Energy Conversion and Management, 97 (2015) 26-41.
[17] R. Kalbasi, M. Afrand, J. Alsarraf, M.-D. Tran, Studies on optimum fins number in PCM-based heat sinks, Energy, 171 (2019) 1088-1099.
[18] M. Hatami, D. Song, D. Jing, Optimization of a circular-wavy cavity filled by nanofluid under the natural convection heat transfer condition, International Journal of Heat and Mass Transfer, 98 (2016) 758-767.
[19] M. Hatami, Nanoparticles migration around the heated cylinder during the RSM optimization of a wavy-wall enclosure, Advanced Powder Technology, 28 (2017) 890-899.

[20] M. Hosseinzadeh, M. Sardarabadi, M. Passandideh-Fard, Energy and exergy analysis of nanofluid based photovoltaic thermal system integrated with phase change material, Energy, 147 (2018) 636-647.
[21] H. Kim, J. Kim, H. Cho, Experimental study on performance improvement of U-tube solar collector depending on nanoparticle size and concentration of Al2O3 nanofluid, Energy, 118 (2017) 1304-1312.
[22] M. Nakhchi, M. Rahmati, Entropy generation of turbulent Cu–water nanofluid flows inside thermal systems equipped with transverse-cut twisted turbulators, Journal of Thermal Analysis and Calorimetry, (2020) 1-10.
[23] M.H. Esfe, H. Hajmohammad, D. Toghraie, H. Rostamian, O. Mahian, S. Wongwises, Multi-objective optimization of nanofluid flow in double tube heat exchangers for applications in energy systems, Energy, 137 (2017) 160-171.
[24] O. Mahian, L. Kolsi, M. Amani, P. Estellé, G. Ahmadi, C. Kleinstreuer, J.S. Marshall, M. Siavashi, R.A. Taylor, H. Niazmand, Recent advances in modeling and simulation of nanofluid flows-Part I: Fundamentals and theory, Physics reports, 790 (2019) 1-48.
[25] M. Sivashankar, C. Selvam, S. Manikandan, S. Harish, Performance improvement in concentrated photovoltaics using nano-enhanced phase change material with graphene nanoplatelets, Energy, (2020) 118408.
[26] L. Qiu, Y. Ouyang, Y. Feng, X. Zhang, Review on micro/nano phase change materials for solar thermal applications, Renewable energy, 140 (2019) 513-538.
[27] I. Sarani, S. Payan, S. Nada, A. Payan, Numerical investigation of an innovative discontinuous distribution of fins for solidification rate enhancement in PCM with and without nanoparticles, Applied Thermal Engineering, 176 (2020) 115017.
[28] B. Kok, Examining effects of special heat transfer fins designed for the melting process of PCM and Nano-PCM, Applied Thermal Engineering, 170 (2020) 114989.
[29] M. Arıcı, E. Tütüncü, Ç. Yıldız, D. Li, Enhancement of PCM melting rate via internal fin and nanoparticles, International Journal of Heat and Mass Transfer, 156 (2020) 119845.
[30] M. Gürtürk, B. Kok, A new approach in the design of heat transfer fin for melting and solidification of PCM, International Journal of Heat and Mass Transfer, 153 (2020) 119671.
[31] C.R. Nóbrega, K.A. Ismail, F.A. Lino, Solidification around axial finned tube submersed in PCM: Modeling and experiments, Journal of Energy Storage, 29 (2020) 101438.
[32] C. Zhao, M. Opolot, M. Liu, F. Bruno, S. Mancin, K. Hooman, Numerical study of melting performance enhancement for PCM in an annular enclosure with internal-external fins and metal foams, International Journal of Heat and Mass Transfer, 150 (2020) 119348.
[33] F.S. dos Santos, K.A. Ismail, F.A. Lino, A. Arabkoohsar, T.G. Lago, Parametric investigation of the enhancing effects of finned tubes on the solidification of PCM, International Journal of Heat and Mass Transfer, 152 (2020) 119485.
[34] F. Li, N. Muhammad, E. Abohamzeh, A.A. Hakeem, M.R. Hajizadeh, Z. Li, Q.-V. Bach, Finned unit solidification with use of nanoparticles improved PCM, Journal of Molecular Liquids, (2020) 113659.
[35] T. Sathe, A. Dhoble, Thermal analysis of an inclined heat sink with finned PCM container for solar applications, International Journal of Heat and Mass Transfer, 144 (2019) 118679.
[36] Z. Khan, Z.A. Khan, P. Sewell, Heat transfer evaluation of metal oxides based nano-PCMs for latent heat storage system application, International Journal of Heat and Mass Transfer, 144 (2019) 118619.

[37] M. Nakhchi, J. Esfahani, Improving the melting performance of PCM thermal energy storage with novel stepped fins, Journal of Energy Storage, 30 (2020) 101424.
[38] C. Ji, Z. Qin, Z. Low, S. Dubey, F.H. Choo, F. Duan, Non-uniform heat transfer suppression to enhance PCM melting by angled fins, Applied Thermal Engineering, 129 (2018) 269-279.
[39] H. Shokouhmand, B. Kamkari, Experimental investigation on melting heat transfer characteristics of lauric acid in a rectangular thermal storage unit, Experimental Thermal and Fluid Science, 50 (2013) 201-212.
[40] A.C. Kheirabadi, D. Groulx, The effect of the mushy-zone constant on simulated phase change heat transfer, ICHMT Digital Library Online, Begel House Inc., 2015.
[41] M. Al-Jethelah, S.H. Tasnim, S. Mahmud, A. Dutta, Nano-PCM filled energy storage system for solar-thermal applications, Renewable energy, 126 (2018) 137-155.
[42] A. Brent, V. Voller, K. Reid, Enthalpy-porosity technique for modeling convection-diffusion phase change: application to the melting of a pure metal, Numerical Heat Transfer, Part A Applications, 13 (1988) 297-318.
[43] S. Deng, C. Nie, G. Wei, W.-B. Ye, Improving the melting performance of a horizontal shell-tube latent-heat thermal energy storage unit using local enhanced finned tube, Energy and Buildings, 183 (2019) 161-173.
[44] A. Abdi, V. Martin, J.N. Chiu, Numerical investigation of melting in a cavity with vertically oriented fins, Applied energy, 235 (2019) 1027-1040.
[45] R. Karami, B. Kamkari, Investigation of the effect of inclination angle on the melting enhancement of phase change material in finned latent heat thermal storage units, Applied Thermal Engineering, 146 (2019) 45-60.
[46] B. Kamkari, D. Groulx, Experimental investigation of melting behaviour of phase change material in finned rectangular enclosures under different inclination angles, Experimental Thermal and Fluid Science, 97 (2018) 94-108.
[47] Y. Xu, M.-J. Li, Z.-J. Zheng, X.-D. Xue, Melting performance enhancement of phase change material by a limited amount of metal foam: Configurational optimization and economic assessment, Applied energy, 212 (2018) 868-880.